Phase Transition Behavior of Two-component Viologen Adsorption Layers on a HOPG Electrode Surface

Yasuhiko Tanaka [a] and Takamasa Sagara [b]*

[a] *Department of Materials Science, Graduate School of Science and Technology, Nagasaki University, Bunkyo 1-14, Nagasaki 852-8521, Japan*

[b] *Department of Applied Chemistry, Faculty of Engineering, Nagasaki University, Bunkyo 1-14, Nagasaki 852-8521, Japan*

---

*Corresponding author.   Tel. & fax: +81 95 8192676;

 E-mail address: sagara@nagasaki-u.ac.jp (T. Sagara)

Abstract

Phase transition behavior of two-component viologen adsorption layers at a HOPG electrode was described using the results of voltammetric measurements. In the coexistence of heptyl viologen (HV) and its bis-carboxylated derivative in the solution phase, a well-mixed condensed monolayer of the radical cations was formed at any molar fraction. In sharp contrast, the binary system of HV and butyl viologen (BV) exhibited phase separation in the molar fraction range where BV is saturated in the predominantly formed condensed phase of HV. It was, however, found that this separation, being opposed to the prediction based on the adsorption free energy, occurs only when the time period enough for full condensation of HV is not given. The significant features of phase transition of two-component viologen adsorption layers on a HOPG electrode surface were highlighted in comparison with the formation and reductive desorption of the self-assembled monolayers of alkanethiols.

1. Introduction

Well mix or separate into domains?　This question is frequently arisen in two-dimensional (2D) binary systems at electrode|solution interfaces, especially in monolayer formation processes on electrode surfaces from two-component adsorbate solutions.　Understanding of the structures and formation processes of 2D binary films is of importance in the fabrication of functional modified electrodes.　The state of the film formed through spontaneous adsorption process from a binary solution may be determined mainly by three factors: (1) thermodynamics of mixing of the two components on the surface to achieve the state of the lowest energy, (2) kinetics of the film formation process, and (3) the sequence of adsorption events.　In other words, we can learn the delicate balance among adsorption free energy, intermolecular interaction, and film formation kinetics from the observation of the adsorption process.

The self-assembled monolayer (SAM) formation of alkanethiols or their derivatives on a metal electrode surface has provided us with an interesting model case of a 2D binary system. The thiol SAM formed through an irreversible adsorption process undergoes reductive desorption at negative potentials in a strong alkaline medium [1], enabling us to answer the question, mix or separate.　Kakiuchi and his coworkers have reported the characteristics of a number of binary alkanethiol SAMs on Au electrodes.　For example, undecanethiol and mercaptoundecanoic acid are well-mixed in the SAM as evidenced by the appearance of reductive desorption voltammetric peak in between the potentials of individuals [2].　When the difference of alkyl chain lengths exceeds two or three in the number of methylene carbons, phase separation into two domains takes place as exemplified by the mixed SAM of hexadecane thiol and mercaptopropionic acid [3].　In this case, two distinct reductive desorption peaks are observed in the voltammogram.　Similar phase separation due to the alkyl chain length difference has been demonstrated by a Monte-Carlo calculation by Shevade and coworkers [4].　As an intriguing case, 2-aminoethanethiol and 2-mercaptoethane sulfonic acid form a stable SAM of 1:1 composition on a Au electrode surface irrespective of the solution composition due to strong lateral electrostatic interaction, demonstrating an ideal nonideality [5].

Viologen molecules bearing two long alkyl chains exhibit 2D phase transition of the first

order upon the redox reaction between dication (V^{2+}) and radical cation ($V^{\bullet+}$) forms when being adsorbed on a basal plane of a highly oriented pyrolytic graphite (HOPG) electrode [6-10].   In cyclic voltammograms (CVs), the phase transition process of viologen gives rise to spike-like peaks at less negative potentials than the potential of the bulk redox reaction [6,7].   The reduction process is the formation of the ordered condensed monolayer of flat-lying $V^{\bullet+}$ molecules from the gas-like adsorption layer of V^{2+} state, while the oxidation is the reverse process.   Arihara and coworkers revealed the facts that $V^{\bullet+}$ moieties in the condensed phase assume the side-on configuration and alkyl chains of $V^{\bullet+}$ molecules orient parallel to the surface from their IR reflection study [6].   Recently, Pham and coworkers have found a stripe pattern of adsorbed $V^{\bullet+}$ form of benzyl viologen on a chloride modified Cu(100) electrode surface by *in situ* STM observations [11].   In the STM image, the main molecular axis is parallel to the surface in a side-on adsorption geometry, exhibiting the formation of π-stacked polymer chains.

In this report, we describe the phase transition features of two-component viologen mixed adsorption layers using the results of CV measurements at a HOPG electrode.   Because the one-component viologen systems at a HOPG electrode show their unique voltammetric transition peak potentials, CV can be used as the footprint of the state of the condensed films also for binary systems.   We demonstrate herein typical two different binary systems.   The occurrence of the phase transition is due to the strong intermolecular interactions of $V^{\bullet+}$ molecules on the HOPG surface.   The interactions include stacking between radical cation moieties, interchain interaction, and edge-to-edge interaction such as hydrogen bonding.   In comparison to the binary SAMs of alkanethiols and their derivatives, we may have two features to be highlighted: (1) both monolayer formation and dissolution processes can be observed directly as voltammetric responses, and (2) the effect of multiple modes of intermolecular interaction upon the film structure can be disclosed, because the interacting molecules are lying flat on the electrode surface as opposed to alkanethiols.

2. Experimental

Scheme 1

N,N'-diheptyl-4,4'-bipyridinium dibromide (heptyl viologen, HV) purchased from TCI was purified by recrystallization. 1,1'-bis(7-carboxyheptyl)-4,4'-bipyridinium dibromide (bis-carboxylated viologen, V-(C_7-COOH)$_2$) was prepared previously [10]. N,N'-dibutyl-4,4'-bipyridinium dibromide (butyl viologen, BV) was synthesized and purified. Molecular structures of three viologen molecules are shown in Scheme 1. Water was purified to its resistibity over 18 MΩ cm. All other chemicals were of reagent grade and used as received. A plate of HOPG (PGX 04: size 12 × 12 × 3 mm-thickness, Panasonic graphite, Matsushita Electric Industrial Co.) was perpendicularly attached with the end of a copper pipe using a carbon paste glue. To expose a fresh basal plane, the surface of the HOPG was peeled off by the use of a Scotch$^®$ adhesive tape immediately before use. The HOPG electrode (electrode area: 1.44 cm^2) was horizontally touched to the Ar gas|viologen solution interface and set in a hanging meniscus configuration.

The base electrolyte solution was 0.3 M KBr. Adjustment of pH was made by adding HBr or KOH. In binary viologen solutions of HV + V-(C_7-COOH)$_2$ and HV + BV, the total concentration of two different viologens was kept constant at 0.1 mM. The molar fraction of HV, x_{HV} was used to represent the mixing ratio in the solution phase. All the electrochemical measurements were made using a Ag|AgCl|sat'd KCl reference electrode and a coiled Au wire counter electrode under an Ar gas (> 99.998 %) atmosphere at 23 ±1°C. To prevent the electrode from exhibiting history effects, the peeling-off procedure of the HOPG electrode was always made when changing of the solution composition.

3. Results and Discussion

3.1. Mixture of HV and V-(C_7-COOH)$_2$ as a typical well-mixing case

Fig. 1   *See page 12*

Fig. 1-A shows the CVs for a HOPG electrode in contact with HV + V-(C_7-COOH)$_2$ mixed solution with various x_{HV}. In the solution containing solely V-(C_7-COOH)$_2$ (curve a), the

cathodic and anodic spike peak potentials were at E_{pc} = –0.51 V and E_{pa} = –0.33 V, respectively. The cathodic peak corresponds to the transition of a gas-like adsorption state of V^{2+} to a 2D condensed phase of $V^{\bullet+}$, accompanied by a one-electron transfer reaction. Anodic peak represents the reversal transition. In the condensed phase, hydrogen bonding interaction is established between V-(C_7-COOH)$_2$ molecules at their both ends on the HOPG electrode at pH 2.1 [10]. In the solution containing solely HV (curve g), peak potentials were E_{pc} = –0.34 V and E_{pa} = –0.30 V. These results are in line with our previous reports [7-10]. The greater peak separation for V-(C_7-COOH)$_2$ than HV is due to the effective positive contribution of hydrogen bonding to the intermolecular attraction in the condensed phase [10].

Typical CVs for various x_{HV} ranging from 0.010 to 0.99 are shown as curves b-f in Fig. 1-A, together with x_{HV} dependence of peak potentials (E_p), the full width at the half-height of the peak ($\Delta W_{1/2,p}$), and peak charge (Q_p) in Figs. 1-B through D.

With an increase of x_{HV} from 0 to 0.4, the peak potentials were unchanged from those for curve a obtained in the presence of solely V-(C_7-COOH)$_2$. Although the increase of $\Delta W_{1/2,p}$ of the cathodic peak was observed, Q_p was unchanged. Note that the value of Q_p for a pure condensed film of V-(C_7-COOH)$_2$ (13 µC cm^{-2}) is smaller than that for a pure condensed film of HV (15 µC cm^{-2}), reflecting the molecular size. These observations indicate that the condensed phase is composed dominantly of reduced V-(C_7-COOH)$_2$ when x_{HV} < 0.4.

When x_{HV} exceeds 0.5, monotonic shifts of both E_{pc} and E_{pa} to less-negative potentials were observed. The pronounced shift of the peak potentials at x_{HV} > 0.8 was in line with the increase of Q_p. The mixing of HV in the condensed film is obvious at x_{HV} > 0.5. However, even at x_{HV} = 0.99 (curve f), E_{pc} was still 53 mV more negative that at x_{HV} = 1, indicating predominant content of V-(C_7-COOH)$_2$ in the condensed film. Note that, in the range of 0.80 < x_{HV} < 0.96, the anodic peak apparently split to two peaks, while the cathodic peak did not. It cannot be denied that, even though the condensation of a two-component film takes place at a single potential upon reduction, two distinct domains in the condensed phase are present in the superficial film. Because the maximum peak splitting was smaller than 25 mV, the difference of the composition of the two domains may be minor.

The intermolecular hydrogen bonding formation between reduced V-(C_7-COOH)$_2$ molecules may provide stronger homo-interaction than the homo-interaction between reduced

HV molecules. Therefore, even though V-(C$_7$-COOH)$_2$ is more soluble in water than HV, the molar fraction of V-(C$_7$-COOH)$_2$ in the condensed film is greater than its solution fraction. To evaluate the significance of hydrogen bonding ability of carboxylated viologen, behavior in alkaline solution was examined.

Fig. 2   *See page 13*

In Fig. 2, CVs for HV + V-(C$_7$-COOH)$_2$ mixture at $x_{HV} = 0.5$ at two far different pH were compared. In alkaline solution (pH 13), the transition peaks appeared at almost the same positions as in the presence of solely HV, indicating that the content of reduced V-(C$_7$-COOH)$_2$ molecule in the condensed phase is negligibly small even at $x_{HV} = 0.5$. In alkaline solution, V-(C$_7$-COOH)$_2$ is deprotonated to be V-(C$_7$-COO$^-$)$_2$, and its intermolecular hydrogen bonding ability is lost. It was confirmed, therefore, that the ability of V-(C$_7$-COOH)$_2$ to form intermolecular hydrogen bonding is the key to form a well-mixed ordered condensed phase as observed in Fig. 1-A. In this phase, HV molecules can mix in without causing disorder of aligned V-(C$_7$-COOH)$_2$ molecules, because the molecular structural difference is only the absence of the end -COOH groups.

3.2. Mixture of HV and BV

Fig. 3   *See page 13*

Fig. 3-A shows typical CVs for HV + BV solutions at a sweep rate of 80 mV s^{-1}. The peak potentials for their one-component systems were at $E_{pc} = -0.44$ V and $E_{pa} = -0.42$ V for BV (curve a) and $E_{pc} = -0.34$ V and $E_{pa} = -0.30$ V for HV (curve g). In the x_{HV} range from unity down to $x_{HV} = 0.091$, only one pair of peaks was observed as exemplified by curves e and f, while negative shift of both E_{pc} and E_{pa} were obviously recorded (Fig. 3-B). When $x_{HV} = 0.062$ was reached, another pair of peaks suddenly appeared at the peak potentials of the one-component system of BV. At lower x_{HV}, the negative shift of the less-negative couple ceased. At $x_{HV} < 0.02$, the peaks of the less-negative couple became too small for the peak

potentials to be read precisely.

In these observations, there are several significant pieces of information to be pointed out.

(1) In the range of $1 > x_{HV} > 0.062$, the tendency of the shift of peak potentials is similar to HV + V-(C_7-COOH)$_2$ binary system. It is likely that BV mixes in the condensed phase whose dominant composition is reduced HV. Only one phase, a well-mixed phase of HV + BV, is present in this range of x_{HV}.

(2) In the process of decreasing x_{HV}, the mixing of reduced BV in the HV-enriched phase reached saturation at $x_{HV} = 0.062$. When $x_{HV} < 0.062$, two domains of condensed monolayer were formed on the HOPG electrode surface, giving rise to two pairs of peaks. The domain originating the peaks at more negative potentials is of nearly pure reduced BV, because the peak potentials, $E_{pc} = -0.44$ V and $E_{pa} = -0.43$ V in the range of $0.01 < x_{HV} < 0.062$ is in accord with those of curve a. The other coexisting domain originating the peaks at less negative potentials is the phase of reduced HV with saturated BV.

(3) At least in the range of $0.025 \leq x_{HV} \leq 0.062$, CV peaks for the two domains coexisted. This fact reveals that the phase of reduced HV with saturated BV does not fully occupy the electrode surface. When sweeping the potential to negative direction, condensation to form the phase of reduced HV with saturated BV undergoes exclusively, followed by the condensation to form the phase of pure BV at more negative potentials. On the basis of the peak charge at $x_{HV} = 0.040$ as an example, the condensation process to create the phase of HV with saturated BV underwent only until it covers approximately 65 % area of the HOPG surface. The residual area remained uncovered until the electrode potential comes to be negative enough to start the condensation of the pure BV phase.

The adsorptivity of HV, bearing longer alkyl chains than BV, should be higher than that of BV. Possible reasons why the condensation of the phase of reduced HV with saturated BV stops growing before the establishment of the full coverage of the electrode surface during the negative potential sweep include: (i) When the content of BV in the phase exceeds a critical limit on the way of the phase growth, the phase is no longer capable of further growing due to the nature of the growing front, (ii) Because the concentration of HV in the solution is low, HV is depleted in the close proximity of the electrode surface to the concentration level that the condensed phase cannot grow furthermore. The reason (i) is a thermodynamic reason, whereas the reason (ii) is the kinetic limitation.

8

If the kinetic limitation is really working, its lifting should facilitate the increase the coverage of the phase of reduced HV with saturated BV.   To see this, the effect of potential-holding was examined.

Fig. 4 shows the results of the potential-holding experiments at x_{HV} = 0.026.   When potential-holding at -0.525 V for a period of 5 minutes was applied (Fig. 4-A), the anodic peak at -0.43 V disappeared, while the anodic peak previously at -0.38 V was shifted to -0.31 V.   Its peak charge became approximately 85% of pure HV condensed phase.   The dependencies on the holding time for the charges of anodic peaks (Q_{pa}), anodic peak potentials (E_{pa}), and total amount of viologen molecules being reoxidized at anodic peaks (Γ_t) are demonstrated in Figs. 4-B through D.   The finally reached E_{pa} value at 5 min was nearly the same as the anodic peak potential for HV one-component system.   The decrease of Q_{pa} of more negative anodic peak was in line with the increase of Q_{pa} of less negative anodic peak. Taken together, during the time period of the potential-holding, displacement of BV phase on the electrode surface by HV takes place.   This reveals that the most stable state at -0.525 V is the full coverage of the condensed phase of HV.   To reach the state, enough time to restore the enough concentration of HV near the electrode surface is needed.   This supports above-mentioned reason (ii).   Additionally, we examined the use of very slow potential sweep rates.   When the rate was as low as 0.8 mV s^{-1}, complete extinction of more negative pair of peaks was observed.   This means that, when the kinetic restriction is lifted, the thermodynamics is the principal determining factor over the sequence of adsorption events.

Additionally, the plot of Γ_t as a function of the holding time (Fig. 4-D) clearly indicates that, as far as BV condensed phase coexists, the HOPG surface is not fully covered by viologens at a sweep rate of 80 mV s^{-1}.   The time period allowed for phase transition affects not only the ratio of two viologens on the surface but also total amount in the condensed phase.

4. Concluding remarks

In this report, we demonstrated two examples of phase transition processes at a HOPG electrode in contact with two-component viologen solutions using the results of voltammetric measurements. In the coexistence of HV and V-(C$_7$-COOH)$_2$ in the solution phase, a well-mixed condensed monolayer of the radical cations was formed at any molar fraction. In sharp contrast, the binary system of HV and BV exhibited phase separation at the lower molar fractions of HV at which BV is saturated in the condensed phase of HV. However, this situation was found to be a transitory state observed only when higher potential sweep rates are used. The finally reached state is the full coverage with the single component HV phase. Interestingly, the time allows the transformation from transitory adsorption state reflecting the adsorption sequence to the thermodynamically most stable state. More detailed studies on other two-component viologen systems are currently underway in our laboratory.

Finally, the characteristic features of binary phase formation on a HOPG electrode surface relevant to this work are worth to be noted in comparison with the reductive desorption of the SAMs of alkanethiol. Only the observation of reduction process has the essential meaning for alkanethiol SAM, while separate observation of both condensation and dissolution processes is allowed for viologen at HOPG. The reoxidation of alkane thiolate never restores the well-defined SAM of alkanethiol. In the case of viologen phase transition at HOPG, appearance of a transitory adsorption state and afterward "place exchange" (and/or "space filling") can be readily monitored repeatedly. The reductive desorption of alkanethiol is a destructive process. The reductive desorption peak area of CV for an alkanethiol SAM cannot be directly equated to the amount of the reduced molecules but calibration for the double layer charging should be made in the light of the shift of apparent pzc [12]. On the other hand, CV peak at a HOPG electrode directly gives the amount of molecule because of the very low double layer capacitance, since a HOPG is a semi-metal [13]. In summary, HOPG|binary-viologen systems may bring about a straightforward view of the state of the condensed monolayer as well as its formation and dissolution processes.

References

[1] C.A. Widrig, C. Chung, M.D. Porter, J. Electroanal. Chem. 310 (1991) 335.

[2] T. Kakiuchi, M. Iida, N. Gon, D. Hobara, S. Imabayashi, K. Niki, Langmuir 17 (2001) 1599.

[3] D. Hobara, M. Ota, S. Imabayashi, K. Niki, T. Kakiuchi, J. Electroanal. Chem. 444 (1998) 113.

[4] A.V. Shevade, J. Zhou, M.T. Zin, S. Jiang, Langmuir 17 (2001) 7566.

[5] Y. Ooi, D. Hobara, M. Yamamoto, T. Kakiuchi, Langmuir 21 (2005) 11185.

[6] K. Arihara, F. Kitamura, K. Nukanobu, T. Ohsaka, K. Tokuda, J. Electroanal. Chem. 473 (1999) 138.

[7] T. Sagara, S. Tanaka, Y. Fukuoka, N. Nakashima, Langmuir 17 (2001) 1620.

[8] T. Sagara, S. Tanaka, K. Miuchi, N. Nakashima, J. Electroanal. Chem. 524-525 (2002) 68.

[9] T. Sagara, K. Miuchi, J. Electroanal. Chem. 567 (2004) 193.

[10] T. Sagara, Y. Fujihara, T. Tada, J. Electrochem. Soc. 152 (2005) E239.

[11] D.-T. Pham, K. Gentz, C. Zörlein, N. T. H. Hai, S.-L. Tsay, B. Kirchner, S. Kossmann, K. Wandelt, P. Broekmann, New J. Chem. 30 (2006) 1439.

[12] T. Kakiuchi, H. Ushi, D. Hobara, M. Yamamoto, Langmuir 18 (2002) 5231.

[13] T. Sagara, M. Fukuda, N. Nakashima, J. Phys. Chem. B 102 (1998) 521.

Scheme and Figures

HV : $H_3C-(CH_2)_6-N^+$ ⬡—⬡ $N^+-(CH_2)_6-CH_3$ ⌉ $2Br^-$

V-(C$_7$-COOH)$_2$: $HOOC-(CH_2)_7-N^+$ ⬡—⬡ $N^+-(CH_2)_7-COOH$ ⌉ $2Br^-$

BV : $H_3C-(CH_2)_3-N^+$ ⬡—⬡ $N^+-(CH_2)_3-CH_3$ ⌉ $2Br^-$
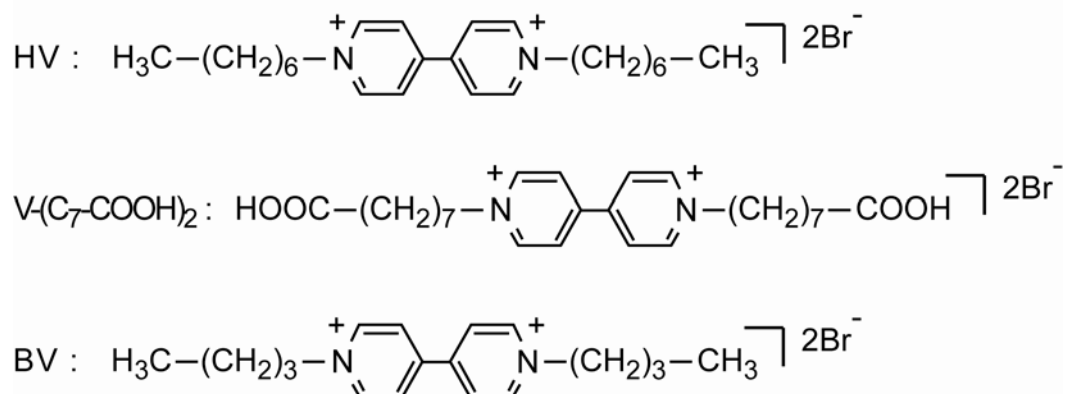
Scheme 1.　Molecular structure of viologens used in this work.
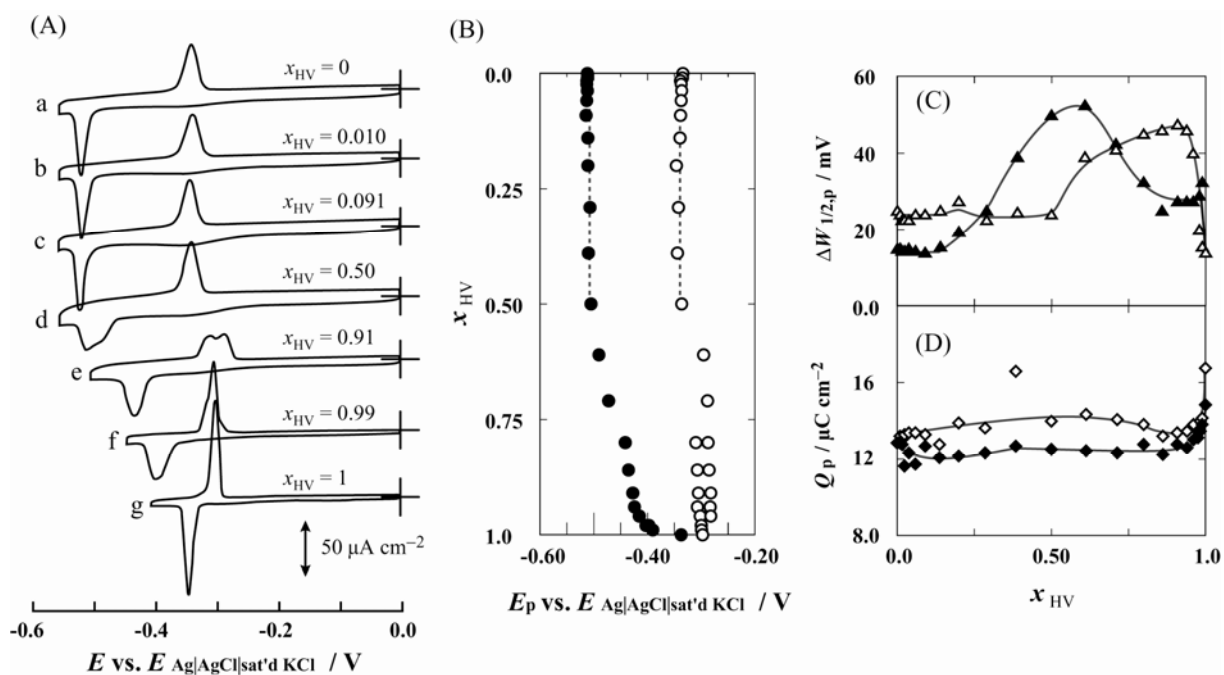
Fig. 1.　A: CVs at a sweep rate of 80 mV s^{-1} for a HOPG electrode in contact with binary solutions of HV and V-(C$_7$-COOH)$_2$ at pH = 2.4 with various molar fractions of HV, x_{HV}: 0 (curve a), 0.010 (curve b), 0.091 (curve c), 0.50 (curve d), 0.91 (curve e), 0.99 (curve f), and 1 (curve g).　Dependencies on x_{HV} were shown for peak potentials (E_p) in B, the full width at the half-height of the peak ($\Delta W_{1/2,p}$) in C, and the peak charge (Q_p) obtained by the integration of the CV curve followed by base-line correction in D.　In B-D, anodic peak data was shown by open symbols, while cathodic one as closed symbols.　The solid lines are added for eye-guides.

12
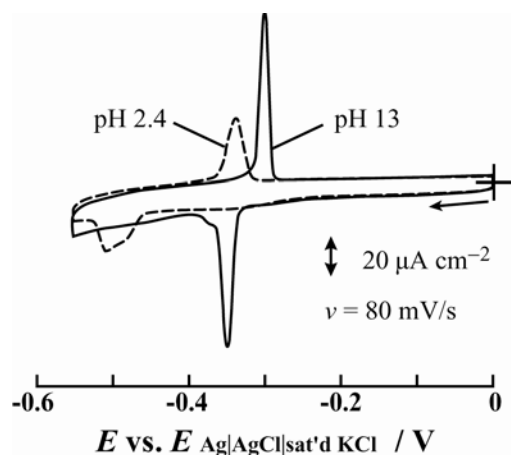
Fig. 2. Comparison of CVs at a sweep rate of 80 mV s^{-1} for HV + V-(C$_7$-COOH)$_2$ ($x_{HV} = 0.5$) at pH = 2.4 and 13. Broken line is the same as curve d in Fig. 1-A.
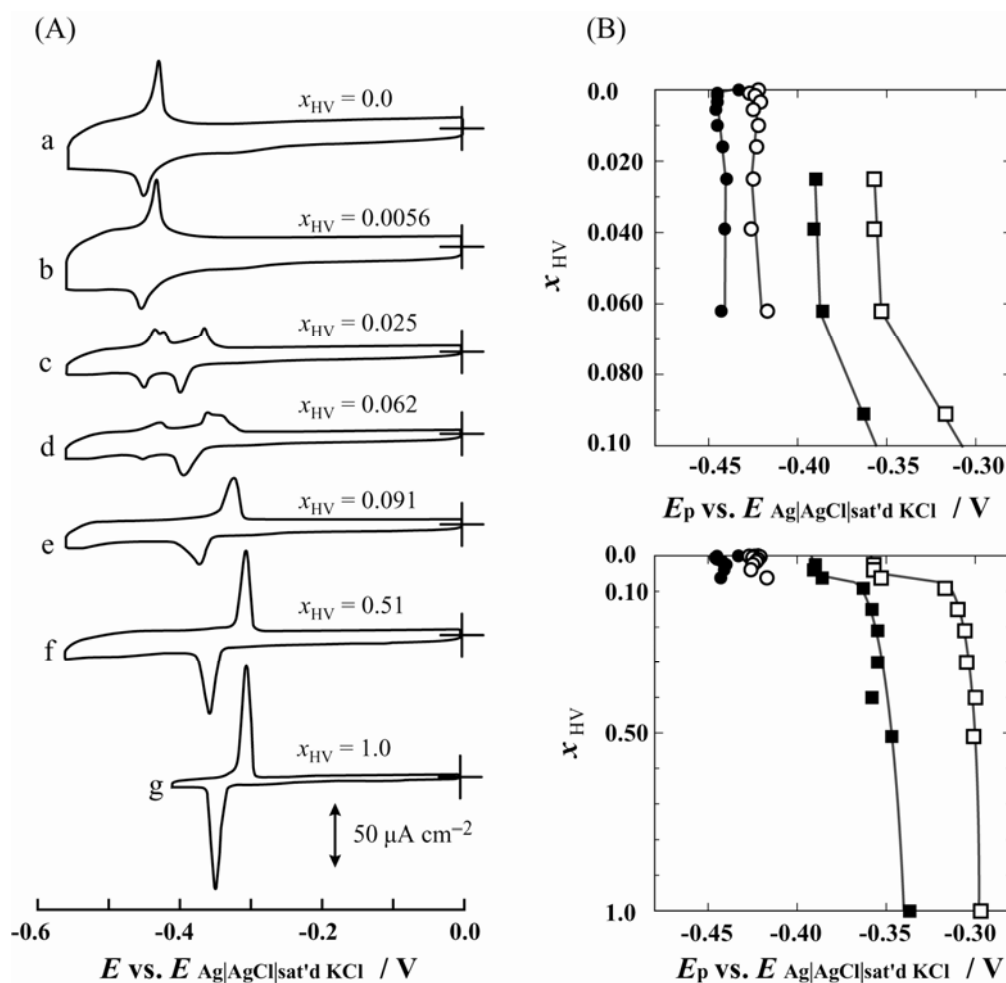
Fig. 3. CVs (A) at a sweep rate of 80 mV s^{-1} and plots of peak potentials (B) for a HOPG electrode in contact with mixed solutions of HV and BV at various ratios. In A, $x_{HV} = 0$ (curve a), 0.0056 (curve b), 0.025 (curve c), 0.062 (curve d), 0.091 (curve e), 0.51 (curve f) and 1.0 (curve g). In B, the upper plot is the closeup of the lower plot. Closed marks represent cathodic peak potentials, and open marks represent anodic ones. The solid lines are added for eye-guides.
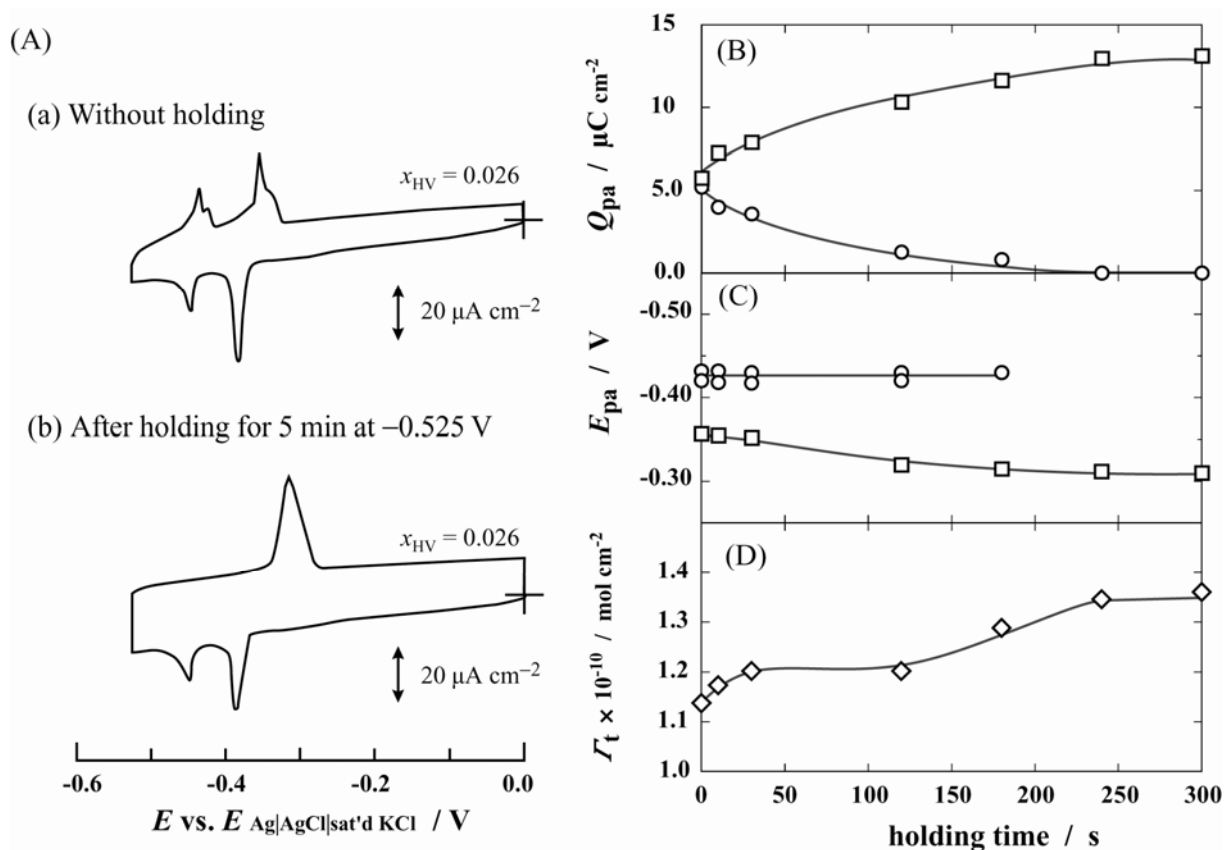
Fig. 4. Results of potential-holding experiments for a HOPG electrode in contact with mixed solutions of HV and BV at $x_{HV} = 0.026$. The sweep rate was 80 mV s^{-1}. In A, CVs without (a) and with (b) potential-holding at -0.525 V for a period of 5 minutes are shown. Dependencies on holding time were shown for the peak charge (Q_{pa}) obtained by the integration of the CV curve followed by base-line correction in B, the anodic peak potentials (E_{pa}) in C, and the total adsorbed amount of viologens (Γ_t) calculated from Q_{pa} in D. The solid lines are added for eye-guides.